P. Gomes
E. Giralt
W. Ochoa
N. Verdaguer
D. Andreu

Probing degeneracy in antigen–antibody recognition at the immunodominant site of foot-and-mouth disease virus

Authors' affiliations:

P. Gomes, Department of Organic Chemistry, University of Barcelona, Barcelona, Spain and C.I.Q. – Centro de Investigação em Química, da Universidade do Porto, Porto, Portugal.

E. Giralt and D. Andreu*, Department of Organic Chemistry, University of Barcelona, Barcelona, Spain; *present address: Department of Experimental and Health Sciences, Pompeu Fabra University, Barcelona, Spain.

W. Ochoa and N. Verdaguer, Barcelona Institute of Molecular Biology – CSIC, Barcelona, Spain.

Correspondence to:

Professor *David Andreu*
Department of Experimental and Health Sciences
Pompeu Fabra University
Doctor Aiguader 80
E-08003 Barcelona
Spain
Tel.: 34-935-422-934
Fax: 34-935-422-934
E-mail: david.andreu@cexs.upf.es

Abstract: Antigen–antibody binding is regarded as one of the most representative examples of specific molecular recognition in nature. The simplistic view of antigenic recognition in terms of a lock-and-key mechanism is obsolete, as it is evident that both antigens and antibodies are flexible and can undergo substantial mutual adaptation. This flexibility is the source of complexities such as degeneracy and nonadditivity in antigenic recognition. We have used surface plasmon resonance to study the effects of combining multiple amino acid replacements within the sequence of the antigenic GH loop of foot-and-mouth disease virus. Our aim was 2-fold: to explore the extent to which antigenic degeneracy can be extended in this particular case, and to search for potential nonadditive effects in introducing multiple amino acid replacements. Combined analysis of one such multiply substituted peptide by SPR, solution NMR and X-ray diffraction shows that antigenic degeneracy can be expected as long as residues directly interacting with the paratope are conserved and the peptide bioactive folding is unaltered.

Abbreviations: 2D-^{1}H NMR, two-dimensional proton nuclear magnetic resonance; AAA, amino acid analysis; AM, 2-[4-aminomethyl-(2,4-dimethoxyphenyl)]phenoxyacetic acid (linker); C_A, analyte concentration; $\Delta\delta H\alpha$, conformational chemical shift for proton α; DIEA, diisopropylethylamine; DMF, *N,N*'-dimethylformamide; EDC, *N*-ethyl-*N*'-dimethylaminopropylcarbodiimide; EDTA, ethylenediaminotetraacetic acid; ESMS, electrospray ionization mass spectrometry; Et$_3$Si, triethylsilane; Fab, fragment antigen binding; FMDV, foot-and-mouth disease virus; Fmoc,

9-fluorenylmethyloxycarbonyl; HPLC, high-performance liquid chromatography; IC$_{50}$, 50% inhibition concentration; k_a, association rate constant (M^{-1}s^{-1}); K$_A$, association thermodynamic constant (M^{-1}); k$_D$, dissociation rate constant (s^{-1}); K$_D$, dissociation thermodynamic constant (M); K$_i$, solution affinity constant (M^{-1}); mAb, monoclonal antibody; MALDI-TOF MS, matrix-assisted laser desorption–time-of-flight mass spectrometry; MBHA, *p*-methylbenzhydrylamine resin; MeCN, acetonitrile; MPLC, medium pressure liquid chromatography; NHS, *N*-hydroxysuccinimide; NMM, *N*-methylmorpholine; NOE, nuclear Overhauser effect; PBS, phosphate buffer saline; OD, optical density; PBS, phosphate buffer saline; R$_{eq}$, equilibrium response; R$_{immob}$, immobilization response; R$_{max}$, maximum response (RU); RU, resonance units; r.p.m., revolutions per minute; SDS–PAGE, sodium dodecyl sulfate–polyacrylamide gel electrophoresis; SPPS, solid-phase peptide synthesis; SPR, surface plasmon resonance; ^{t}Bu, *tert*-butyl; TBTU, 2-(1H-benzotriazole-1-yl)-1,1,3,3-tetramethyluronium tetrafluoroborate; TFA, trifluoroacetic acid; TFE, 2,2,2-trifluoroethanol.

Antigen–antibody binding is regarded as one of the most representative examples of specific molecular recognition in nature (1). The exquisite specificity of immune reactions is not only one of the pillars of host defense, but also the basis for many helpful therapeutic and biotechnological applications. The early, simplistic view of antibody–antigen interactions taking place via lock-and-key mechanisms (2) is inaccurate, as both antigens and antibodies are known to be flexible and able to undergo considerable mutual adaptation (3,4). Because epitope–paratope recognition operates at the atomic rather than at the amino acid residue or sequence level (5–7), a given epitope can be recognized by antibodies devoid of sequential homology in their paratopes (8) and, conversely, an antibody can recognize different epitopes (e.g. peptides) that share little or no sequential similarity (9). An additional example of complexity in antigen–antibody recognition is the occasional observation of nonadditivity, i.e. full recognition of multiple mutants combining deleterious replacements or vice versa (10).

In our work with foot-and-mouth disease virus (FMDV) (11,12), we have encountered examples of a relatively broad recognition of variant peptides by antibodies (10,13–18). These peptides were based on the main antigenic site of FMDV, termed site A, located on the highly flexible GH loop defined by residues 136–150 of the capsid protein VP1 in FMDV isolate C-S8c1 (19). This loop is effectively mimicked by peptide A15 (YTASARGDLAHLTTT), which has been

used in several studies on antigenic structure of this viral site (13,20–22). Site A combines hypervariable segments (137–140 148–150) with highly conserved residues such as Leu^{144} and Leu^{147} and, especially, the integrin-binding motif RGD, used as FMDV cell attachment site (20,21,23). This duality makes site A an extremely interesting ground for testing the boundaries of antigenic recognition. Systematic studies carried out by Valero (24) have shown that amino acid replacements at highly sensitive zones, such as the RGD triplet, are mostly deleterious. In contrast, five single point substitutions (Thr^{137} → Ile, Ala^{138} → Phe, Ala^{140} → Pro, Gly^{142} → Ser and Thr^{148} → Ile) were found to preserve antigenicity towards several anti-GH loop mAbs. Although the first and last replacements are located at each end of the loop, not in close contact with the antibody (22), the other three are at positions known to be directly involved in antibody recognition. Each of these three replacements is also remarkable because of its non-conservative character: Phe is much larger than Ala; Pro is a known disrupter of secondary structure, which Ala is not; finally, the Gly^{142} → Ser mutation affects the highly conserved RGD motif. Studying the effect that every possible combination of these five mutations has on antigenicity provides a feasible way to explore the relative limits of antigenic degeneracy at this particular site. In addition, previous evidence of positive nonadditivity in multiple substitutions within the GH loop (10,13,16–18) encouraged us to look for possible synergistic effects in the simultaneous combination of these amino acid replacements. Therefore, we analyzed the 31 peptides (Table 1) corresponding to the combination of the five mutations by surface plasmon resonance (SPR) (25,26) against three anti-GH loop mAbs with epitope specificities outlined in Fig. 1. The SPR technique was used to quantitate the antibody–peptide solution affinities, using Fab fragments instead of whole mAb so that we could ensure that all complexes had a 1:1 stoichiometry. The new multiply substituted peptides turned out to be comparable with or even better than the native antigen A15 in reactivity against the mAbs. In addition, some positive nonadditivity towards two of the three mAbs under study was observed for peptides containing the Gly^{142} → Ser replacement. Both nuclear magnetic resonance (NMR) and X-ray diffraction (Ochoa *et al.*, manuscript in preparation) data on one of the multiply substituted peptides suggest that the structural features of the multiple mutant are similar to those of the wild-type sequence. These results, together with our previous studies on other multiply substituted FMDV peptides (16–18) provide strong evidence for antigen–antibody flexibility

Table 1. **General data on the synthetic peptides under study**

Peptide	Sequence	Yield (%)[a]	Purity (%)[b]	MW (MH⁺, Da)[c]	AAA composition[d]
A15Scr, negative control	RAGTATTLADLHYST	87	94	1577.7 (1578)	Asp, 1.03; Ser, 0.96; Gly, 1.01; Ala, 3.07; Leu, 1.98; His, 0.93
A15, GH loop of FMDV, isolate C-S8c1	YTASARGDLAHLTTT	93	98	1577.6 (1578)	Asp, 1.12; Ser, 0.98; Gly, 1.06; Ala, 3.00; Leu, 1.95; Tyr, 0.96
A15(^{137}I)	-I-------------	89	99	1589.2 (1589)	Asp, 1.07; Ser, 1.04; Gly, 1.08; Ala, 3.10; Leu, 1.96; His, 0.92
A15(^{138}F)	--F------------	65	97	1653.3 (1653)	Asp, 0.96; Ser, 0.96; Gly, 1.03; Ala, 2.05; Leu, 2.05; His, 0.99
A15(^{140}P)	----P----------	84	98	1603.1 (1603)	Asp, 1.04; Ser, 0.97; Gly, 1.05; Ala, 2.07; Leu, 1.96; Arg, 1.01
A15(^{142}S)	------S--------	79	99	1607.2 (1607)	Asp, 1.05; Ser, 1.99; Ala, 3.08; Leu, 2.00; His, 0.92; Arg, 0.95
A15(^{148}I)	-----------I--	87	98	1589.1 (1589)	Asp, 1.05; Ser, 1.01; Gly, 1.04; Ala, 3.03; Leu, 1.86; Arg, 0.94
A15(^{137}I,^{138}F)	-IF-----------	15	93	1665.1 (1665)	Asp, 1.00; Ser, 0.98; Gly, 1.03; Ala, 1.98; Leu, 1.98; His, 1.02
A15(^{137}I,^{140}P)	-I--P---------	55	91	1615.6 (1615)	Asp, 1.06; Ser, 1.00; Gly, 1.10; Ala, 1.93; Pro, 0.99; Arg, 1.02
A15(^{137}I,^{142}S)	-I----S--------	79	90	1619.2 (1619)	Asp, 0.99; Ser, 2.07; Ala, 3.08; Leu, 2.03; His, 0.88; Arg, 0.95
A15(^{137}I,^{148}I)	-I---------I--	78	97	1601.3 (1601)	Asp, 1.00; Ser, 0.99; Gly, 1.01; Ala, 3.04; His, 0.92; Arg, 0.99
A15(^{138}F,^{140}P)	--F-P---------	72	95	1679.6 (1679)	Asp, 1.06; Pro, 1.01; Gly, 1.09; Ala, 1.05; Leu, 1.89; Arg, 1.07
A15(^{138}F,^{142}S)	--F---S--------	86	89	1684.1 (1684)	Asp, 1.05; Ser, 2.10; Ala, 2.05; Leu, 1.88; His, 0.92; Arg, 1.00
A15(^{138}F,^{148}I)	--F--------I--	86	91	1665.4 (1665)	Asp, 1.03; Ser, 0.95; Gly, 1.03; Ala, 2.00; His, 0.90; Arg, 1.09
A15(^{140}P,^{142}S)	----P-S--------	81	87	1632.4 (1633)	Asp, 1.02; Pro, 1.03; Ala, 2.04; Leu, 1.93; His, 0.92; Arg, 1.11
A15(^{140}P,^{148}I)	----P-------I--	79	89	1615.6 (1615)	Asp, 1.03; Ser, 0.95; Gly, 1.00; Ala, 2.01; His, 0.95; Arg, 1.07
A15(^{142}S,^{148}I)	------S-----I--	79	86	1619.6 (1619)	Asp, 1.05; Ser, 1.96; Ala, 3.10; Tyr, 0.87; His, 0.92; Arg, 1.14
A15(^{137}I,^{138}F,^{140}P)	-IF-P---------	78	94	1691.6 (1691)	Asp, 1.03; Ser, 0.96; Gly, 1.05; Ala, 1.01; Pro, 0.98; Arg, 1.05
A15(^{137}I,^{138}F,^{142}S)	-IF---S--------	95	86	1694.5 (1695)	Asp, 1.10; Ser, 1.90; Tyr, 0.91; Phe, 1.01; His, 0.97; Arg, 1.08
A15(^{137}I,^{138}F,^{148}I)	-IF--------I--	83	95	1677.4 (1677)	Asp, 1.01; Ser, 0.91; Gly, 1.01; Ala, 1.97; His, 1.07; Arg, 1.04
A15(^{137}I,^{140}P,^{142}S)	-I--P--S-------	82	94	1644.3 (1645)	Asp, 1.03; Pro, 1.04; Ala, 2.01; Leu, 1.90; His, 0.91; Arg, 1.12
A15(^{137}I,^{140}P,^{148}I)	-I--P-------I--	71	92	1626.6 (1627)	Asp, 1.05; Ser, 0.99; Gly, 1.08; Ala, 1.93; Pro, 1.00; Arg, 1.03
A15(^{137}I,^{142}S,^{148}I)	-I----S-----I--	80	92	1631.1 (1631)	Asp, 1.05; Ser, 2.07; Ala, 2.97; Leu, 1.84; His, 0.96; Arg, 0.95
A15(^{138}F,^{140}P,^{142}S)	--F-P-S--------	73	97	1708.3 (1709)	Asp, 0.97; Ser, 1.97; Ala, 1.04; Leu, 2.08; Phe, 1.03; Arg, 1.02
A15(^{138}F,^{140}P,^{148}I)	--F--P------I-	87	90	1690.1 (1691)	Asp, 1.02; Pro, 1.00; Gly, 1.06; Ala, 1.02; Phe, 0.86; His, 0.90
A15(^{138}F,^{142}S,^{148}I)	--F---S-----I--	88	91	1695.0 (1695)	Asp, 1.07; Tyr, 0.87; Phe, 0.91; Ala, 2.09; Leu, 1.85; His, 1.07
A15(^{140}P,^{142}S,^{148}I)	----P-S----I--	89	92	1645.0 (1645)	Asp, 1.00; Pro, 1.02; Tyr, 0.93; Ala, 2.02; Arg, 1.11; His, 0.91
A15(^{137}I,^{138}F,^{140}P,^{142}S)	-IF-P-S--------	77	95	1720.9 (1721)	Asp, 0.98; Ser, 1.91; Pro, 0.98; Ala, 0.99; Arg, 1.07; His, 1.07
A15(^{137}I,^{138}F,^{140}P,^{148}I)	-IF-P-------I--	74	94	1703.1 (1703)	Asp, 0.99; Ser, 0.94; Gly, 1.03; Ala, 0.96; Pro, 0.96; Arg, 1.01
A15(^{137}I,^{138}F,^{142}S,^{148}I)	-IF---S-----I--	84	98	1706.7 (1707)	Asp, 1.07; Ser, 2.06; Arg, 0.89; Ala, 2.04; Leu, 1.91; His, 0.93
A15(^{137}I,^{140}P,^{142}S,^{148}I)	-I--P-S-----I--	80	91	1656.0 (1657)	Asp, 1.02; Ser, 1.91; Pro, 1.02; Ala, 1.98; Arg, 1.11; His, 0.96
A15(^{138}F,^{140}P,^{142S},^{148}I)	--F-P-S-----I--	56	92	1721.2 (1721)	Asp, 1.04; Ser, 2.01; Pro, 1.04; Ala, 1.01; Phe, 0.91; Arg, 1.08
A15(^{137}I,^{138}F,^{140}P,^{142}S,^{148}I)	-IF-P-S-----I--	80	94	1732.1 (1733)	Asp, 1.09; Ser, 2.03; Pro, 1.02; Ala, 1.05; Leu, 1.99; Arg, 0.95

a. Global yield: synthesis plus purification.
b. As percentage of peak area in HPLC.
c. Determined by either MALDI-TOF or ESI methods; theoretical mass in parenthesis.
d. Results for the six best matching residues in each hydrolysate. Contiguous Thr and Ile are known to hydrolyse nonquantitatively under standard conditions.

underlying degeneracy in antigenic recognition. For GH loop peptides, in particular, recognition seems to rely on strict conservation of those atoms directly interacting with paratope groups, while allowing for a certain sequence diversity in the rest of the sequence, as long as the bioactive folding is preserved.

Results

Peptides

Thirty-three 15-residue peptides (Table 1) were synthesized, one representing site A of FMDV C-S8c1 (A15), another as

$$^{136}\text{Y T A S A R G D L A H L T T }^{150}\text{T}$$
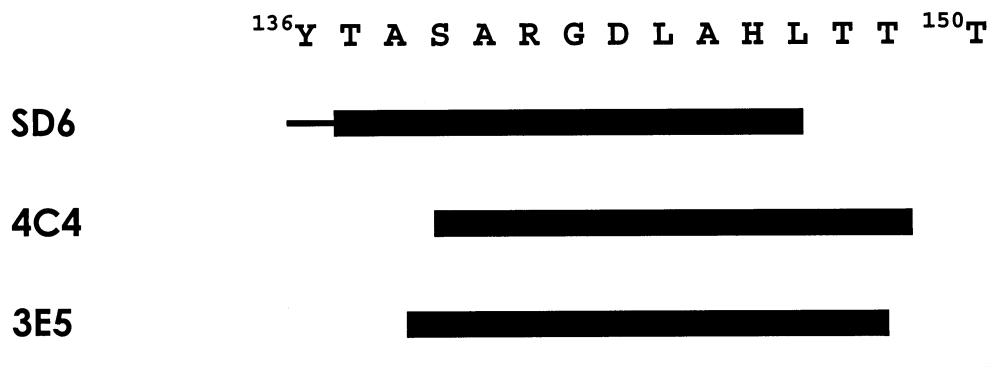
SD6

4C4

3E5

Figure 1. Specificity of the anti-GH loop mAbs assayed. The minimal location of SD6, 4C4 and 3E5 epitopes, as deduced by studies with synthetic peptides and variant viruses, is shown by a thick line; a thinner line indicates some effect on binding of the corresponding residues.

a negative control with scrambled sequence (A15Scr), and 31 other sequences corresponding to all possible (one-, two-, three-, four- and five-point) combinations of the mutations under analysis. All peptides were synthesized using Fmoc solid-phase methods (27) with high yields ($\approx 80\%$), purified (>90% by HPLC) and satisfactorily identified (AAA, ESMS, MALDI-TOF MS) as the target sequences.

Solution affinity SPR analysis

The viability of direct kinetic biosensor analysis of the interactions between immobilized anti-FMDV mAbs and soluble 15-residue peptides has been previously demonstrated (14,15,17,18,28). In this study, however, most interactions could not be described kinetically, because of high association rates, extremely slow dissociation rates or incomplete surface regeneration (not shown). Deviations from the ideal behavior (29) could be detected, thus affecting true binding kinetics. Alternative indirect SPR approaches (i.e. surface competition with a high molecular mass analyte) (30) did not provide reliable means to study the kinetics of the peptide–antibody interactions because of inadequacy of the high molecular mass antigens assayed (Gomes *et al.*, unpublished data).

The inability to obtain kinetic data on the peptide–mAb systems under study led us to the alternative solution affinity approach. In the particular case of antigen–antibody interactions, it must be ensured that reactions take place at a 1:1 stoichiometry. Thus, instead of whole immunoglobulins, Fab fragments produced by standard papain digestion were employed. Injection of known Fab (SD6, 4C4 and 3E5) standards on the A15 surface allowed the building of initial binding rate vs. Fab concentration calibration curves (17,18), which were subsequently used

in the quantitation of Fab molecules that remained free after overnight incubation with peptide antigens in solution.

Determination of the remaining free Fab in solution for each incubated mixture (where Fab total concentration was constant and peptide antigen concentrations varied) allowed us to build inhibition curves (Fig. 2) from which the peptide–antibody solution affinities were calculated using the Cheng & Prusoff's formula (eqn 1) (31). Results are summarized in Table 2 and confirm the high peptide–antibody affinities expected in view of the avidity effects observed in the kinetic SPR analyses. These high peptide antigenicities were in agreement with a competition ELISA screening of these peptides using the same anti-GH loop mAbs (Gomes *et al.*, unpublished data) and with the avidity effects observed in the initial kinetic approach.

The multiply substituted peptides displayed antigenicities that generally correlated with additive effects in the combination of the different amino acid replacements (Fig. 3), with an interesting systematic exception: peptides including the Gly$^{142} \rightarrow$ Ser replacement vs. mAbs 4C4 and 3E5.

Affinity data

SPR screening of the substituted peptides showed the one-point mutants to be closely equivalent in terms of antigenicity (Table 2). Nonetheless, Ala$^{138} \rightarrow$ Phe and Gly$^{142} \rightarrow$ Ser replacements negatively affected recognition by mAb SD6; the second replacement, which involves the RGD motif, was also disfavored by the other two mAbs. The involvement of Ala^{138} in peptide–SD6 complexes (22) and the important role of the RGD triplet are both in agreement with previous observations (21,22,32,33). However, all mAbs were fully reactive with Thr$^{137} \rightarrow$ Ile and
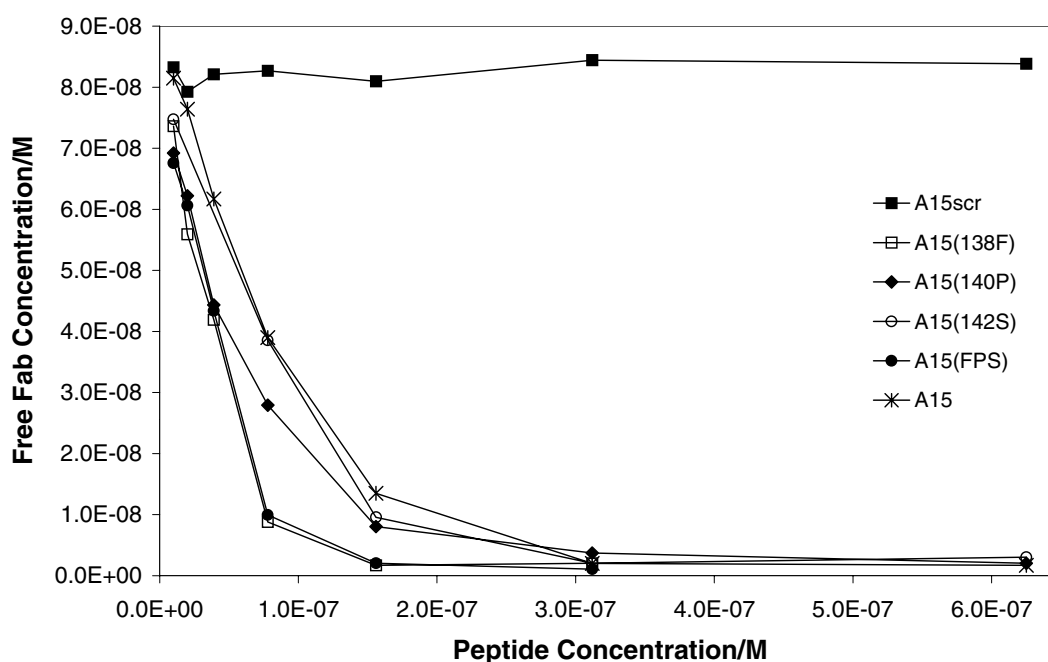
Figure 2. Variation of remaining free Fab at equilibrium (total [Fab]=80 nM) with competitor peptide concentration (from 0 to 600 nM). For clarity, only inhibition curves for Fab 4C4 vs. peptides A15, A15Scr, A15(138F), A15(140P), A15(142S) and A15(138F,140P,142S) are displayed.

Thr[148] → Ile replacements, which is consistent with the minimal participation of these residues in mAb–peptide interaction, as seen by X-ray diffraction studies (16,21; Ochoa *et al*., manuscript in preparation).

The multiply substituted peptides displayed, in general, similar antigenicities (Table 2), in agreement to what was expected from additive effects in the combination of the one-point mutations (Fig. 3). However, for mAbs 4C4 and 3E5, affinities of multiple mutants containing the Gly[142] → Ser replacement were systematically higher than expected from the 'additivity rule'. Such deviations suggest a small positive synergistic effect in these multiple mutants.

Two-dimensional ¹H NMR study of peptide A15(138F,140P,142S)

The absolute conformational chemical shifts for peptide A15(138F,140P,142S) (Fig. 4) are comparable with those previously observed for the native peptide A15 (34,35). The global shape of the plots resembles those observed for other GH loop peptides under identical conditions (34,35). The region containing the open turn centered at the Arg-*Ser*-Asp triplet is followed by an incipient helix, as usually observed for other FMDV peptides (34,35). Moreover, the almost identical plots obtained in either water or 30% TFE (Fig. 4) suggest that the multiply substituted peptide is not particularly sensitive to structure-inducing solvents, and

thus is conformationally stable. These findings are further supported by the observation of a few (weak but informative) $NN_{i,i+1}$ and $NN_{i,i+2}$-type NOEs (not shown), consistent with the nascent helical path in the Ser[142]–His[146] region mentioned above.

Discussion

Anti-GH loop mAbs have previously been reported to display higher than expected reactivities towards multiply substituted FMDV peptides (10,13). This positive non-additivity has been attributed to peptide folding properties, where less favorable conformational effects caused by a given amino acid replacement could be compensated by introduction of additional residue substitutions, leading to the recovery of the bioactive folding pattern (Fig. 5A) (16). Our results similarly suggest that the decrease in affinity provoked by the Gly[142] → Ser replacement in the 141–143 open turn is adequately counterbalanced by substitutions outside this region. Indeed, when the triply substituted A15(138F,140P,142S) peptide was studied in solution using 2D ¹H NMR, conformational features similar to those characterizing the native A15 could be detected. Further, the antigenically relevant open-turn motif centered at the R*S*D triplet was conformationally stable and involved a higher number of residues than in the wild-type peptide,

Table 2. Association binding constants from solution affinity SPR

Peptide[a]	$K_i^{c,d}/M^{-1}$ mAb SD6	$K_i^{c,d}/M^{-1}$ mAb 4C4	$K_i^{c,d}/M^{-1}$ mAb 3E5
A15Scr[b]	–	–	–
A15	6.3×10^7	2.0×10^8	2.0×10^8
A15(^{137}I)	**8.5×10^7**	2.0×10^8	*1.4×10^8*
A15(^{138}F)	*3.6×10^7*	2.1×10^8	2.1×10^8
A15(^{140}P)	7.1×10^7	1.8×10^8	1.6×10^8
A15(^{142}S)	*2.7×10^7*	*7.3×10^7*	*6.2×10^7*
A15(^{148}I)	6.7×10^7	2.0×10^8	2.0×10^8
A15(IF)	5.1×10^7	2.2×10^8	*1.6×10^8*
A15(IP)	6.1×10^7	2.1×10^8	*1.3×10^8*
A15(IS)	5.2×10^7	1.9×10^8	*1.3×10^8*
A15(II)	**9.1×10^7**	2.3×10^8	2.0×10^8
A15(FP)	*2.8×10^7*	2.2×10^8	2.0×10^8
A15(FS)	*7.1×10^6*	2.0×10^8	*1.6×10^8*
A15(FI)	*2.1×10^7*	2.1×10^8	1.9×10^8
A15(PS)	*3.6×10^7*	2.0×10^8	*6.2×10^7*
A15(PI)	6.0×10^7	1.8×10^8	1.9×10^8
A15(SI)	*1.6×10^7*	1.9×10^8	*1.2×10^8*
A15(IFP)	7.4×10^7	2.2×10^8	1.9×10^8
A15(IFS)	*2.0×10^7*	*8.5×10^7*	*5.9×10^7*
A15(IFI)	5.6×10^7	**2.4×10^8**	1.8×10^8
A15(IPS)	7.4×10^7	2.2×10^8	*1.4×10^8*
A15(IPI)	**7.9×10^7**	2.2×10^8	2.0×10^8
A15(ISI)	4.5×10^7	2.2×10^8	*1.7×10^8*
A15(FPS)	*6.5×10^6*	2.1×10^8	*1.3×10^8*
A15(FPI)	5.0×10^7	*1.3×10^8*	1.8×10^8
A15(FSI)	*1.3×10^7*	2.1×10^8	*1.5×10^8*
A15(PSI)	*2.5×10^7*	2.1×10^8	*1.5×10^8*
A15(IFPS)	4.7×10^7	2.2×10^8	*1.3×10^8*
A15(IFPI)	7.1×10^7	2.0×10^8	1.8×10^8
A15(IFSI)	*1.9×10^7*	2.1×10^8	*1.2×10^8*
A15(IPSI)	5.0×10^7	*1.5×10^8*	*1.3×10^8*
A15(FPSI)	*1.7×10^7*	2.2×10^8	*1.3×10^8*
A15(IFPSI)	*3.8×10^7*	1.9×10^8	1.7×10^8

a. Peptide abbreviated names are presented, with only the single-letter codes of the mutated residues being shown; full peptide sequences are displayed in Table 1;
b. As depicted in Fig. 2, binding of negative control peptide (A15Scr) to mAbs could not be detected;
c. K_i (association binding constants) calculated from experimental data (inhibition curves as depicted in Fig. 5) by application of the Cheng & Prusoff's formula (see text);
d. K_i values >20% higher than K_i(A15) are shown in bold; K_i values >10% lower than K_i (A15) are shown in italics.

ranging from the non-native Pro[140] to Leu[147]. This turn-stabilizing effect of the Ala[140] → Pro replacement has also been observed in a parallel X-ray diffraction study of the complex between Fab 4C4 and this mutant peptide (Ochoa

et al., manuscript in preparation). This diffraction study furnished valuable additional information regarding the other two replacements: (i) the aromatic ring of Phe[138] points outwards of the peptide pseudo-cycle (Fig. 5A), engaging in hydrophobic interactions with the mAb binding pocket and not disrupting intrapeptide interactions; (ii) the side-chain hydroxyl of Ser[142] effectively replaces the water molecule present in complexes of mAbs with (native) [142]Gly-containing peptides. Either the water molecule or the Ser hydroxyl contribute to an intrapeptide hydrogen bond network connecting main chain heteroatoms of residues 139 and 144 (Figs 5B,C).

In conclusion, our study of this family of peptides from the FMDV immunodominant site reinforces previous evidence (17,18,28) that antigenicity is compatible with substantial sequence variability in peptides based on the GH loop, provided two key requisites are fulfilled: (i) residues involved in direct epitope–paratope contacts (Arg[141], Asp[143], Leu[144], His[146]) must be conserved; (ii) conformationally important residues may be replaced by others equally able to engage in intrapeptide interactions promoting the bioactive conformation, i.e. a quasicyclic folding supported by interactions between N-terminal Ala[138], Ser[139] and C-terminal Leu[144,147] residues, respectively. Amino acid replacements that not only do not disrupt, but also help to promote these essential requirements can yield variant peptides with significant reactivity towards anti-FMDV neutralizing mAbs, altogether providing a significant example of degeneracy in antigen-antibody recognition mechanisms.

Materials and methods

Peptide synthesis and purification

Peptides (Table 1) were prepared as C-terminal carboxamides using solid-phase methods in an AMS 422 multiple peptide synthesizer (Abimed, Germany) using Fmoc/^{t}Bu chemistry on an AM-MBHA resin (Novabiochem, 0.51 mmol/g). The synthesis was performed at a 0.025-mmol scale, using 20% piperidine (Aldrich) in DMF (Scharlau) for Fmoc deprotection. Couplings were carried out with 4 eq. of Fmoc-amino acid (Bachem), 4 eq. of TBTU (Neosystem) and 8 eq. of NMM (Merck) for 1 h. Peptides were cleaved from the resin and deprotected by treatment with 1 mL of TFA (Kalichemie)/Et$_3$SiH (Aldrich)/H$_2$O (95:2.5:2.5 v/v/v) for 2 h. The crude peptides were precipitated from the TFA solution by treatment with cold
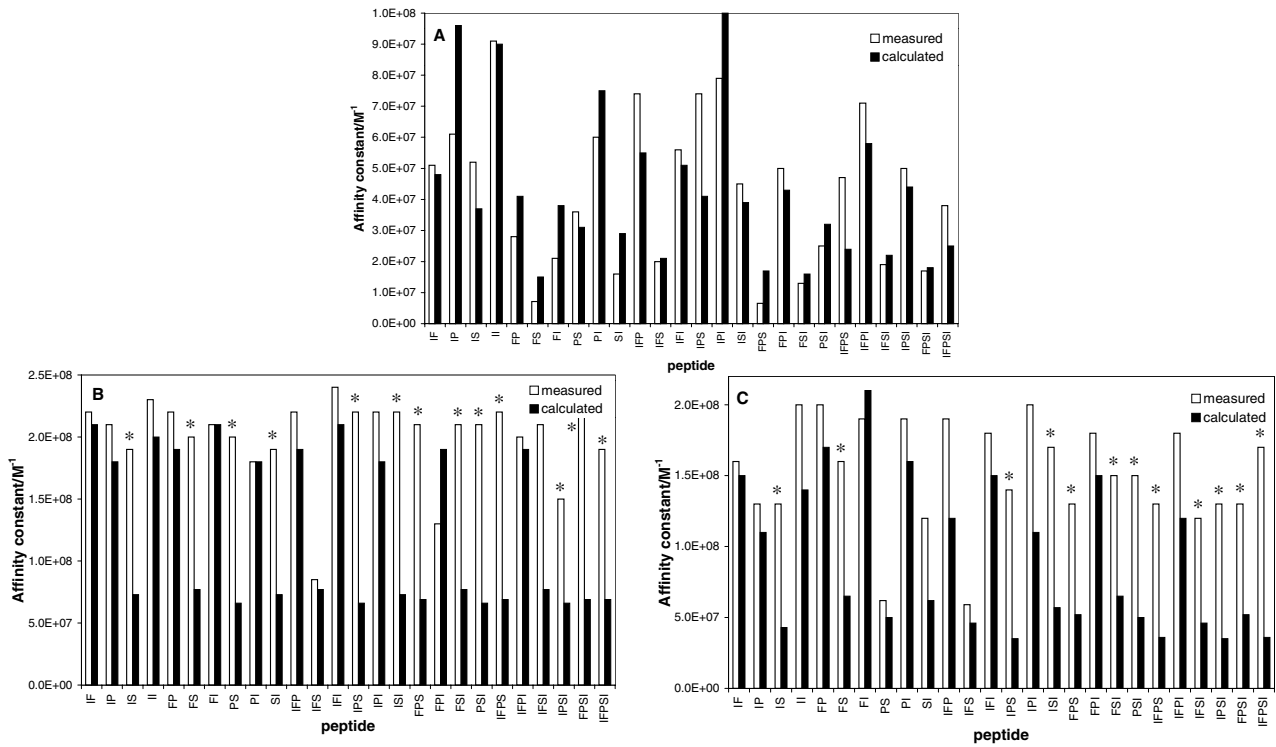
Figure 3. Comparison between measured and calculated affinities (K_i) assuming additive effects on the combinations of the different amino acid replacements: Fab fragments of mAbs (A) SD6, (B) 4C4 and (C) 3E5. (a) Calculated K_i (multiple-mutant peptide, e.g. with mutations 1, 2 and 4)=K_{rel} (single-mutant 1)×K_{rel} (single-mutant 2)×K_{rel} (single-mutant 4)×K_i (peptide A15), where K_{rel}=measured K_i (single-mutant x)/measured K_i (reference peptide A15). (b) Peptide nomenclature has been changed for conciseness: each peptide is named after the single letter codes of the residues replacing native ones. Thus, FSI stands for A15(138F,142S,148I). (c) Peptides giving affinities higher than expected from additivity calculations are marked with an asterisk.
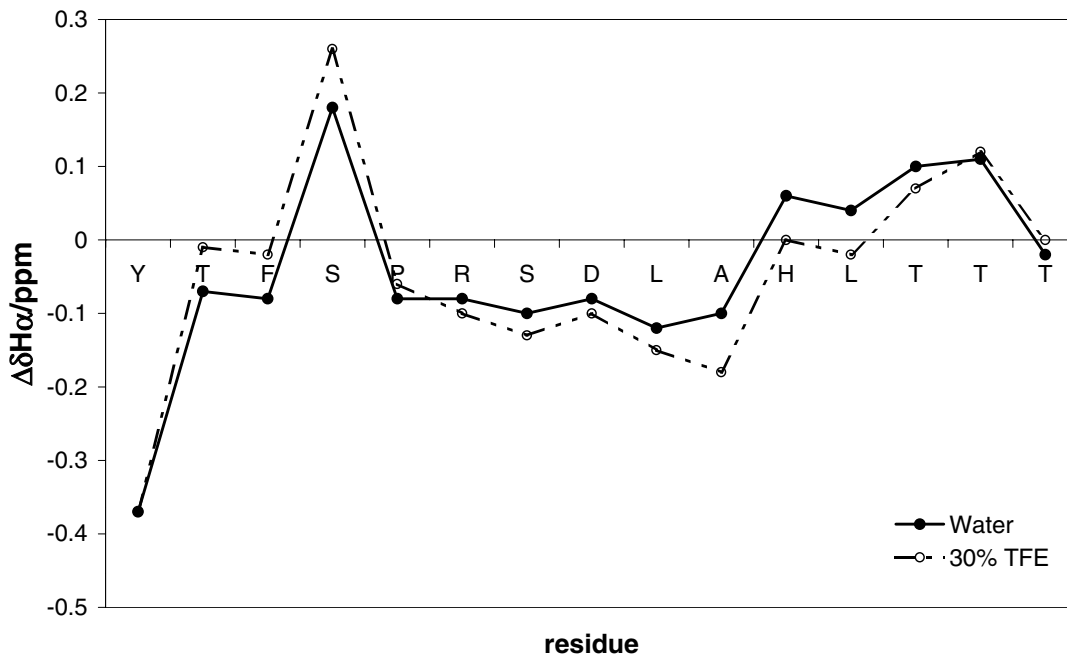
Figure 4. Conformational chemical shift plots ($\Delta\delta H\alpha$) from the 2D ^{1}H NMR analysis of peptide A15(138F,140P,142S) in water and in 30% TFE.
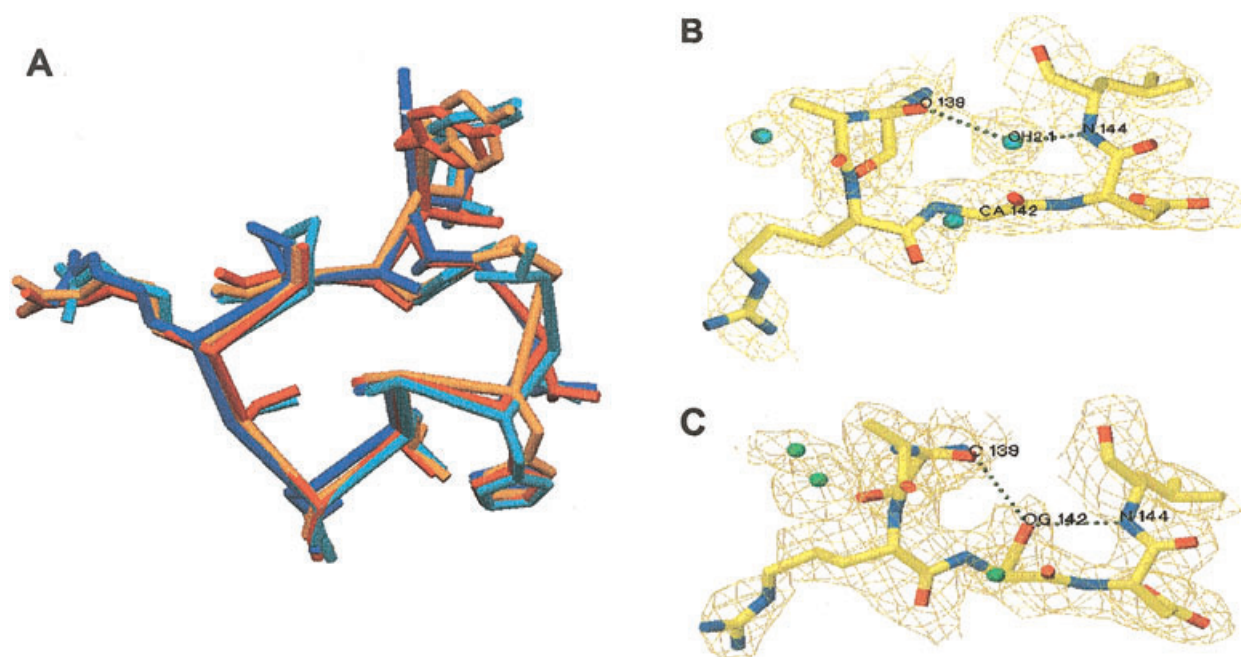
Figure 5. (A) Superimposed structures of multiply substituted peptides in complex with Fab 4C4. (B) Detail of the native RGD loop (note the water molecule bridging residues 139 and 144). (C) Detail of the mutated RSD loop (note the side chain OH group of Ser[142] bridging residues 139 and 144). These graphic representations of structures from crystallographic data were processed using the SETOR program (42).

tert-butyl methyl ether (Fluka), redissolved in 10% acetic acid (Merck), lyophilized and purified by reverse-phase liquid chromatography, using a linear $5 \rightarrow 25\%$ gradient of MeCN (Scharlau) in water with 0.05% TFA on a Vydac C_{18} reverse phase column (250×25 mm, 15–20 µm, 300 Å). Purified peptides were satisfactorily characterized by AAA (Beckman 6300), HPLC (Waters or Shimadzu instruments; Nucleosil C_{18} columns, 250×4 mm, 5 µm, 120 Å) and ESMS (Fisons VG Quattro) or MALDI-TOF MS (Brucker II Biflex).

Solutions for SPR analysis

Peptide stock solutions, ≈ 2.5 mM in 0.1 M acetic acid, were prepared and quantitated by AAA. Solutions for BIAcore analysis were obtained by 1000-fold and subsequent serial dilutions in HBS. Stock solutions of mAbs SD6 and 4C4 (supplied by Dr Esteban Domingo, Center for Molecular Biology, Madrid, Spain), in PBS with 0.02% sodium azide, pH 7.3, were quantitated using the Pierce BCA assay. mAb 3E5 was purified from ascitic fluid (supplied by Dr Emiliana Brocchi; Istituto Zooprofilattico, Brescia, Italy) using a HiTrap Protein A affinity column (Pharmacia Biotech) and quantitated spectrophotometrically (1 OD_{280}=0.75 mg/mL).

For solution affinity SPR assays, PBS solutions (≈ 16 mg/mL) of the Fab fragments. The Fab fragments were kindly provided by Dr Esteban Domingo, except for Fab 3E5, which was prepared by papain digestion as follows. mAb 3E5 was purified from ascitic fluid as described above and concentrated by precipitation with 45% ammonium sulfate; the suspension was centrifuged (10000 r.p.m., 4°C) for 20 min and pellet was resuspended in the minimum volume of PBS and dialyzed overnight against PBS (3×1 L). Antibody (3 mg in 2 mL of PBS) and papain (30 µg in 24 µL 0.1 M EDTA, 126 µL 100 mM cysteine) solutions were mixed, diluted to 3 mL and incubated at 37°C for 5 h; the reaction was quenched with iodoacetamide (80 µL) and the digest was analyzed by SDS–PAGE on a 12% acrylamide gel, using mAb and Fab 4C4 as standards. Proteins in the digest were precipitated with 85% ammonium sulfate and centrifuged (4°C, 10000 r.p.m.) for 20 min; pellet was resuspended in minimal volume of 1:1 PBS/buffer A (112.4 g/L glycine, 175.4 g/L NaCl, pH 8.9 adjusted with NaOH), dialyzed overnight against buffer A (3×1 L); centrifuged at 12000 r.p.m. (4°C) to remove remaining solid particles, and eluted through a protein A–Sepharose column. Fractions with $OD_{280} \geq 0.5$ (first elution peak) were pooled and concentrated to a final volume of 2 mL using a Centriprep-3 concentrator (Amicon) at 2000 r.p.m.; Fab 3E5 was filtered through Sephadex G-100 in PBS (20 mL/h; 4°C); protein-containing fractions (monitored at 280 nm) were pooled, concentrated (Centriprep-3) and quantitated by optical density at 280 nm.

Solution affinity SPR analysis

A sensor chip surface containing the wild-type peptide A15 was prepared according to the manufacturer's instructions: a 5-μL/min HBS continuous flow was maintained and the carboxymethyl surface was activated by a 7-min injection of a solution containing 0.2 M EDC and 0.05 M NHS. A15 surfaces were obtained by injecting 35 μL of a 200 μg/mL A15 solution in 10 mM sodium acetate buffer, pH 5.5. Unreacted activated groups were blocked by a 6-min injection of ethanolamine and remaining noncovalently bound molecules were washed off with a 3-min pulse of 50 mM HCl. The final immobilization response was ≈260 RU, corresponding to a high surface peptide density (0.26 ng/mm²) that favors mass-transport limitations (36). Different solutions of Fab in HBS with known concentrations were injected over the A15 sensor chip surface at 5 μL/min and initial binding rates (proportional to analyte concentration under diffusion-controlled kinetics) were measured from the slopes of the sensorgrams at earlier stages of the injection (at about the 100th second, to avoid influence from initial bulk refractive index 'jumps'). The calibration curve initial binding rate vs. Fab concentration was built and fitted to a 4-parameter equation using the BIAEVALUATION 3.0.2 software. This equation was then used to calculate free Fab concentrations on subsequent assays.

Peptide–Fab interactions were studied by overnight incubation at 4°C of varying peptide concentrations with a constant 80 nM total Fab concentration in HBS, followed by SPR quantitation of the remaining free Fab at equilibrium. Fab–peptide mixtures were allowed to re-equilibrate at 25°C, prior to injection on the A15 surface for Fab quantitation. Free Fab dependence on peptide concentration was plotted and the affinity binding constant K_i was calculated using the Cheng & Prusoff's formula (31):

$$K_i = \frac{1 + K_A[Fab]}{IC_{50}} \qquad (1)$$

where IC_{50} is the concentration of peptide competitor giving a 50% decrease in Fab concentration and K_A is the immobilized peptide A15–antibody affinity previously measured by direct kinetic SPR analysis (14,15,17,18).

Two-dimensional ¹H RMN of peptide A15(138F,140P,142S)

Spectra were acquired at 25°C, both in aqueous solution (85% H_2O+15% D_2O) and in the presence of the structure-promoting agent TFE (30% TFE+60% H_2O+10% D_2O) at a peptide concentration of 2 mM, with 1,4-dioxane added as an internal reference. All experiments were carried out on a Varian VXR-500S NMR spectrometer and further processed with the VNMR software programs. The 2D ¹H NMR (37) experiments performed were (i) TOCSY (38) (70 ms mixing time), (ii) NOESY (39) (200 or 400 ms mixing time), and (iii) ROESY (40) (200 ms mixing time). Water signal elimination was carried out either upon presaturation or using the WATERGATE (41) method. Prior to the Fourier transform, both FIDs and interferograms were multiplied by an exponential function.

References

1. Abbas, A.K., Lichtman, A.H. & Pober, J.S. (2000) *Cellular and Molecular Immunology*. WB Saunders, New York.

2. Mariuzza, R.A., Phillips, S.E.V. & Poljak, R.J. (1987) The structural basis of antigen–antibody recognition. *Annu. Rev. Biophys. Biophys. Chem.* **16**, 139–159.

3. Bhat, T.N., Bentley, G.A., Fischmann, T.O., Boulot, G. & Poljak, R.J. (1990) Small rearrangements in structures of Fv and Fab fragments of antibody D1.3 on antigen binding. *Nature* **347**, 483–485.

4. Wilson, I.A. & Stanfield, R.L. (1994) Antibody–antigen interactions: new structures and new conformational changes. *Curr. Opin. Struct. Biol.* **4**, 857–867.

5. Berzofsky, J.A. (1985) Intrinsic and extrinsic factors in protein antigenic structure. *Science* **229**, 932–940.

6. Van Regenmortel, M.H.V., ed. (1992) *Structure of Antigens*, Vol. 1. CRC Press, Boca Raton, FL.

7. Van Regenmortel, M.H.V. & Muller, S. (1999) *Synthetic Peptides as Antigens*. Elsevier, Amsterdam.

8. Lescar, J., Pellegrini, M., Souchon, H., Tello, D., Poljak, R.J., Peterson, N., Greene, M. & Alzari, P.M. (1995) Crystal structure of a cross-reaction complex between Fab F9.13.7 and guinea fowl lysozyme. *J. Biol. Chem.* **270**, 18067–18076.

9. Geysen, H.M., Rodda, S.J., Mason, T.J., Tribbick, G. & Schoofs, P.G. (1987) Strategies for epitope analysis using peptide synthesis. *J. Immunol. Methods* **102**, 259–274.

10. Mateu, M.G., Andreu, D., Carreño, C., Roig, X., Cairó, J., Camarero, J., Giralt, E. & Domingo, E. (1992) Non-additive effects of multiple amino acid substitutions on antigen-antibody recognition. *Eur. J. Immunol.* **22**, 1385–1389.

11. Pereira, H.G. (1981) Foot-and-mouth disease virus. In: *Virus Diseases of Food Animals* (Gibbs, R.P.J., ed.). Academic Press, New York.

12. Domingo, E., Mateu, M.G., Martínez, M.A., Dopazo, J., Moya, A. & Sobrino, F. (1990) Genetic variability and antigenic diversity of foot-and-mouth disease virus. In: *Applied Virology Research: Virus Variation and Epidemiology* (Kurstak, E., Marusyk, R.G., Murphy, S.A. & Van Regenmortel, M.H.V., eds). Plenum Press, New York.

13. Carreño, C., Roig, X., Cairó, X., Camarero, J., Mateu, M.G., Domingo, E., Giralt, E. & Andreu, D. (1992) Studies on antigenic variability of C-strains of foot-and-mouth disease virus by means of synthetic peptides and monoclonal antibodies. *Int. J. Peptide Protein Res.* **39**, 41–47.

14. Gomes, P., Giralt, E. & Andreu, D. (2000) Direct single-step surface plasmon resonance analysis of interactions between small peptide analytes and immobilised monoclonal antibodies. *J. Immunol. Methods* **325**, 101–111.

15. Gomes, P., Giralt, E. & Andreu, D. (2000) Surface plasmon resonance screening of synthetic peptides mimicking the immunodominant region of C-S8c1 foot-and-mouth disease virus. *Vaccine* **18**, 362–370.

16. Ochoa, W.F., Kalko, S.G., Mateu, M.G., Gomes, P., Andreu, D., Domingo, E., Fita, I. & Verdaguer, N. (2000) A multiply substituted GH loop from foot-and-mouth disease virus in complex with a neutralising antibody: a role for water molecules. *J.Gen. Virol.* **81**, 1495–1505.

17. Gomes, P., Giralt, E. & Andreu, D. (2001) Antigenicity modulation upon peptide cyclization: application to the GH loop of foot-and-mouth disease virus strain C_1-Barcelona. *Vaccine* **19**, 3459–3466.

18. Gomes, P., Giralt, E. & Andreu, D. (2000) Surface plasmon resonance study of synthetic peptides from foot-and-mouth disease virus: effects of cyclization on antigen recognition. In: *Peptides 2000* (Martínez, J. & Feherentz, J.A., eds). EDK, Paris, pp. 639–640.

19. Mateu, M.G., Martínez, M.A., Capucci, L., Andreu, D., Giralt, E., Sobrino, F., Brocchi, E. & Domingo, E. (1990) A single amino acid substitution affects multiple overlapping epitopes in the major antigenic site of foot-and-mouth disease virus of serotype C. *J. Gen. Virol.* **71**, 629–637.

20. Mateu, M.G., Valero, M.L., Andreu, D. & Domingo, E. (1996) Systematic replacement of amino acid residues within an Arg-Gly-Asp containing loop of foot-and-mouth disease virus and effect on cell recognition. *J. Biol. Chem.* **271**, 12814–12819.

21. Verdaguer, N., Mateu, M.G., Andreu, D., Giralt, E., Domingo, E. & Fita, I. (1995) Structure of the major antigenic loop of foot-and-mouth disease virus complexed with a neutralizing antibody: direct involvement of the Arg-Gly-Asp motif in the interaction. *EMBO J.* **14**, 1690–1696.

22. Verdaguer, N., Sevilla, N., Valero, M.L., Stuart, D., Brocchi, E., Andreu, D., Giralt, E., Domingo, E., Mateu, M.G. & Fita, I. (1998) A similar pattern of interaction for different antibodies with a major antigenic site of foot-and-mouth disease virus: implications for intratypic antigenic variation. *J. Virol.* **72**, 739–748.

23. Fox, G., Parry, N.R., Barnett, P.V., McGinn, B., Rowlands, D.J. & Brown, F. (1989) The cell attachment site on foot-and-mouth disease virus includes the amino acid sequence RGD (arginine-glycine-aspartic acid). *J. Gen. Virol.* **70**, 625–637.

24. Valero, M.L. (1997) Mimetización estructural e inmunogénica del sitio antigénico principal del virus de la fiebre aftosa. PhD Dissertation, University of Barcelona, Barcelona.

25. Fägerstam, L.G., Frostel-Karlsson, Å., Karlsson, R., Persson, B. & Rönnberg, I. (1992) Biospecific interaction analysis using surface plasmon resonance detection applied to kinetic, binding site and concentration analysis. *J. Chromatogr.* **597**, 397–410.

26. Schuck, P. (1997) Use of SPR to probe the equilibrium and dynamic aspects of interactions between biological macromolecules. *Annu. Rev. Biophys. Biomol. Struct.* **26**, 541–566.

27. Fields, G.B. & Noble, R.L. (1990) 9-Fluorenylmethoxycarbonyl amino acids in solid phase peptide synthesis. *Int. J. Peptide Protein Res.* **35**, 161–214.

28. Gomes, P., Giralt, E. & Andreu, D. (2001) Molecular analysis of peptides from the GH loop of foot-and-mouth disease virus C-S30 using surface plasmon resonance: a role for kinetic constants. *Mol. Immunol.* in press.

29. Hall, D.R., Cann, J.R. & Winzor, D.J. (1996) Demonstration of an upper limit to the range of association rate amenable to study by biosensor technology based on SPR. *Anal. Biochem.* **235**, 175–184.

30. Karlsson, R. (1994) Real-time competitive kinetic analysis of interactions between low-molecular-weight ligands in solution and surface-immobilised receptors. *Anal. Biochem.* **221**, 142–151.

31. Lazareno, S. & Birdsall, N.J. (1993) Estimation of competitive antagonist affinity from functional inhibition curves using the Gaddum, Schild and Cheng-Prusoff equations. *Br. J. Pharmacol.* **109**, 1110–1119.

32. Mateu, M.G. (1995) Antibody recognition of picornaviruses and escape from neutralization: a structural view. *Virus Res.* **38**, 1–24.

33. Domingo, E., Verdaguer, N., Ochoa, W.F., Ruiz-Jarabo, C.M., Sevilla, N., Baranowski, E., Mateu, M.G. & Fita, I. (1999) Biochemical and structural studies with neutralising antibodies raised against foot-and-mouth disease virus. *Virus Res.* **62**, 169–175.

34. Haack, T., Camarero, J.A., Roig, X., Mateu, M.G., Domingo, E., Andreu, D. & Giralt, E. (1997) A cyclic disulfide peptide reproduces in solution the main structural features of a native antigenic site of foot-and-mouth disease virus. *Int. J. Biol. Macromol.* **20**, 209–219.

35. Valero, M.L., Camarero, J.A., Haack, T., Mateu, M.G., Domingo, E., Giralt, E. & Andreu, D. (2000) Native-like cyclic peptide models of a viral antigenic site: finding a balance between rigidity and flexibility. *J. Mol. Recog.* **13**, 5–13.

36. O'Shannessy, D.J. & Winzor, D.J. (1996) Interpretation of deviations to pseudo-first-order kinetic behaviour in the characterisation of ligand binding by biosensor technology. *Anal. Biochem.* **236**, 275–283.

37. Wüthrich, K. (1986) *NMR of Proteins and Nucleic Acids*. Wiley, New York.

38. Braunschweiler, L. & Ernst, R.R. (1983) Coherence transfer by isotropic mixing: application to proton correlation spectroscopy. *J. Magn. Reson.* **53**, 521–528.

39. Kumar, A., Ernst, R.R. & Wüthrich, K. (1980) A two-dimensional nuclear Overhauser enhancement (2D NOE) experiment for the elucidation of complete proton–proton cross-relaxation networks in biological macromolecules. *Biochem. Biophys. Chem. Commun.* **95**, 1–6.

40. Bothner-By, A.A., Stephens, R.L., Lee, J., Warren, C.D. & Jeanloz, R.W. (1984) Structure determination of a tetrasaccharide: transient nuclear Overhauser effects in the rotating frame. *J. Am. Chem. Soc.* **106**, 811–813.

41. Piotto, M., Saudek, V. & Sklenár, V. (1992) Gradient-tailored excitation for single-quantum NMR spectroscopy of aqueous solutions. *Biomol. NMR* **2**, 661–665.

42. Evans, S.V. (1993) SETOR: hardware-lighted three-dimensional solid model representations of macromolecules. *J. Mol. Graphics* **11**, 134–138.